forests

MDPI

Article

Error Analysis on the Five Stand Biomass Growth Estimation Methods for a Sub-Alpine Natural Pine Forest in Yunnan, Southwestern China

Guoqi Chen [1,2], Xilin Zhang [1,2], Chunxiao Liu [1,2], Chang Liu [1,2], Hui Xu [1,2] and Guanglong Ou [1,2,*]

[1] College of Forestry, Southwest Forestry University, Kunming 650224, China
[2] Key Laboratory of State Forestry Administration on Biodiversity Conservation in Southwest China, Southwest Forestry University, Kunming 650224, China
* Correspondence: olg2007621@swfu.edu.cn

Abstract: Forest biomass measurement or estimation is critical for forest monitoring at the stand scale, but errors among different estimations in stand investigation are unclear. Thus, the *Pinus densata* natural forest in Shangri-La City, southwestern China, was selected as the research object to investigate the biomass of 84 plots and 100 samples of *P. densata*. The stand biomass was calculated using five methods: stand biomass growth with age (SBA), stem biomass combined with the biomass expansion factors (SB+BEF), stand volume combined with biomass conversion and expansion factors (SV+BCEF), individual tree biomass combined with stand diameter structure (IB+SDS), and individual tree biomass combined with stand density (IB+SD). The estimation errors of the five methods were then analyzed. The results showed that the suitable methods for estimating stand biomass are SB+BEF, M+BCEF, and IB+SDS. When using these three methods (SB+BEF, SV+BCEF, and IB+SDS) to estimate the biomass of different components, wood biomass estimation using SB+BEF is unsuitable, and root biomass estimation employing the IB+SDS method was not preferred. The SV+BCEF method was better for biomass estimation. Except for the branches, the mean relative error (MRE) of the other components presented minor errors in the estimation, while MRE was lower than other components in the range from −0.11%–28.93%. The SB+BEF was more appealing for branches biomass estimation, and its MRE is only 0.31% lower than SV+BCEF. The stand biomass strongly correlated with BEF, BCEF, stand structure, stand age, and other factors. Hence, the stand biomass growth model system established in this study effectively predicted the stand biomass dynamics and provided a theoretical basis and practical support for accurately estimating forest biomass growth.

Keywords: above-ground biomass; biomass growth; error analysis; *Pinus densata* forests

check for updates

Citation: Chen, G.; Zhang, X.; Liu, C.; Liu, C.; Xu, H.; Ou, G. Error Analysis on the Five Stand Biomass Growth Estimation Methods for a Sub-Alpine Natural Pine Forest in Yunnan, Southwestern China. *Forests* **2022**, *13*, 1637. https://doi.org/10.3390/f13101637

Academic Editor: Giorgio Vacchiano

Received: 7 August 2022
Accepted: 3 October 2022
Published: 6 October 2022

Publisher's Note: MDPI stays neutral with regard to jurisdictional claims in published maps and institutional affiliations.

Copyright: © 2022 by the authors. Licensee MDPI, Basel, Switzerland. This article is an open access article distributed under the terms and conditions of the Creative Commons Attribution (CC BY) license (https://creativecommons.org/licenses/by/4.0/).

1. Introduction

The forest is fundamental to the global carbon cycle and plays a vital role in maintaining the global greenhouse gas balance [1–5]. Biomass data is the basis for studying forestry and ecological problems, and accurately estimating biomass is an essential issue in forest management and forestry research [6–8]. Primarily due to global warming and the carbon dioxide fixed by plants in photosynthesis, accurately measuring the biomass of tree components (wood, bark, branches, leaves, and roots) has attracted significant research attention [9]. Thus, forest biomass measurement, estimation, and growth at the stand scale are crucial to analyzing forest carbon.

Measuring or estimating the stand biomass mainly includes direct harvesting, volume conversion, and biomass equation methods. The harvesting method was first developed, where the biomass of each component is directly obtained by cutting and weighing all trees or estimating the biomass by directly measuring the biomass of the standard trees [10]. The direct harvesting method is characterized by high precision but requires a lot of human

and material resources while causing unavoidable damage to the forest and the environment [11]. This method is not allowed when estimating large-scale forest biomass. In this case, the volume conversion and biomass equation methods are applicable [12]. The volume conversion method can be conducted due to the significant correlation between the stand volume and biomass, [13–16], which is the recommended biomass estimation technique by the Intergovernmental Panel on Climate Change (IPCC) [17,18]. This technique mainly includes biomass expansion factors (BEF) and biomass conversion and expansion factors (BCEF). Nevertheless, using a constant BEF or BCEF does not provide an accurate estimate of forest biomass as they are related to stand density, stand age, and site conditions [19–22]. Therefore, the biomass conversion factor continuous function method was used to improve and achieve better results [23–26]. Moreover, the biomass equation at the stand scale is a standard method to estimate the total or difficult-to-measure stand biomass by easily measurable forest variables [27–29].

Biomass growth models can describe changes in an individual tree or stand size over time [9]. These models can be divided into individual tree growth, stand diameter structure, and whole stand models [30]. More than 3000 biomass models exist [31], where usually, the independent model variables are common factors in forest surveys, such as diameter at breast height (DBH), tree height (H), and age. Moreover, site quality, stand density, and management measurements are incorporated into the growth models to improve their prediction accuracy or analyze the environmental effects. Among them, biomass equations only using the independent variable DBH or both independent variables DBH and H are widely used at the individual tree or stand scale [32–34]. Moreover, the individual tree models incorporating the aging variable are established to describe biomass growth [22,35].

Moreover, when the structure and dynamics of the stand can be described in more detail [36], the growth of the stand can be simulated based on the individual tree model [37–40]. The whole-stand model usually provides a well-behaved output at the stand level but lacks information about the stand's structure [41]. Connecting individual trees and the stand level includes constraint parameters, disaggregation, and combination methods [42]. Although these methods are widely used to connect individual trees and stand levels [43–45], the errors in estimating the stand biomass using the individual tree biomass growth combined with the stand structure are almost not quantified [41,45–47].

In summary, there are many methods for measuring forest biomass and growth, but the estimation accuracy is uncertain, especially estimation from an individual tree to the stand scale [41,45,46]. The estimation methods are logically equivalent, which means that differences between methods may be due to random or non-random processes related to sampling and modeling. Especially the estimation error of these methods is unclear for the various biomass components [46]. Thus, quantifying and comparing the estimation accuracy differences between different methods has essential theoretical and practical significance for accurately describing forest biomass growth.

In this study, the *Pinus densata* natural forest in Shangri-La was used as the research subject to analyze the accuracy differences in estimating stand biomass growth for the different components using five methods. Namely, the stand biomass growth with age (SBA), stand biomass growth with age (SBA), the stem biomass combined with the biomass expansion factors (SB+BEF), the stand volume combined with biomass conversion and expansion factors (SV+BCEF), the individual tree biomass combined with stand diameter structure (IB+SDS), and individual tree biomass combined with stand density (IB+SD). The significant contributions of this work were:

(1) To quantify the error of the different estimation methods for each biomass component;
(2) To establish a stand biomass growth model system;
(3) To explore the applicable estimation methods for forest biomass growth under different conditions.

2. Materials and Methods

2.1. Estimation Methods

Stand biomass is predictable by using the individual tree data indirectly or stand data directly, and the stand biomass growth can be estimated employing both data types. In this study, we designed five estimation methods based on different original data to predict forest biomass growth (Figure 1). As illustrated in Figure 1, as the stand biomass of different components was obtained, the stand biomass model with the stand age (SBA) could be constructed to predict forest biomass growth. The stem biomass data is relatively easy to measure or investigate compared with the other components. The growth models that combined stem biomass data with BEF (SB+BEF) could predict the change of the stand biomass using the stand age. Moreover, the stand volume (SV) was one of the essential variables to describe the forest production and characteristics and, therefore, has gained attraction. Alternatively, the stand volume combined with the change of the BCEF (SV+BCEF) could also predict the stand's biomass growth.

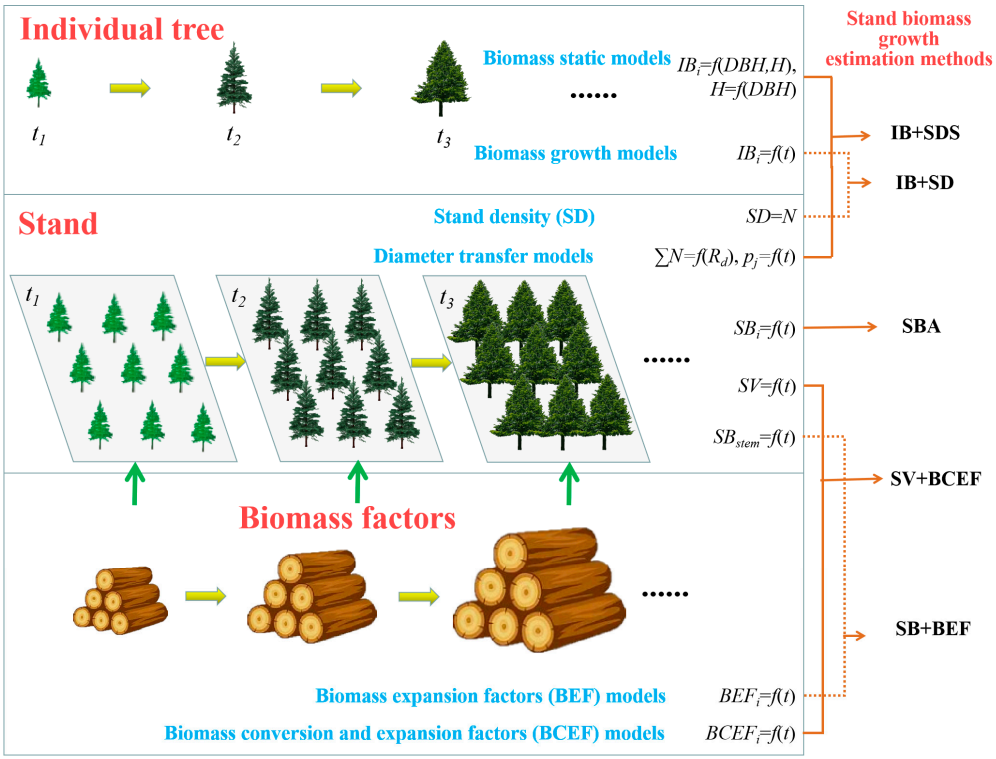


Figure 1. The list of stand biomass growth estimation models. SBA is a direct estimation using stand biomass of the components; SB+BEF is an estimation method using stand stem biomass incorporating BEF_i; SV+BCEF is an estimation method using stand volume incorporating $BCEF_i$; IB+SDS is an estimation method using static biomass of the components for individual tree incorporating dynamical estimation on stand diameter structure; IB+SD is an estimation method using biomass growth of the components for individual tree incorporating stand density. Furthermore, IB_i is the *i*-th components biomass of individual tree; SB_i is the *i*-th components biomass of stand; BEF_i is the biomass expansion factors of the *i*-th components based on stem biomass of stand; $BCEF_i$ is the biomass conversion and expansion factors of *i*-th components biomass based on stand volume; SV is the stand volume; DBH is the diameter at breast height; R_d is the diameter classes; *t* is the age of the tree or stand; SD is the stand density (trees·ha^{-1}); *N* is the cumulative probability of the diameter classes from minimum class; p_j is the estimation of the cumulative probability distribution functions for fitting the stand diameter structure.

Moreover, individual tree biomass and stand structure could also estimate the stand biomass. Indeed, as the individual tree static biomass model was established, the growth of

the stand biomass could be predicted by combining the individual static biomass models with the stand diameter structure dynamic change (IB+SDS). If the biomass growth models of the individual tree had been constructed, this method combined with the individual tree biomass growth model and stand density (IB+SD) could be used to predict the stand biomass growth.

2.2. Study Area

The *Pinus densata* forest in Shangri-La City in the Northwest Yunnan province, Southwest China, was selected as the research object (Figure 2). The geographical coordinates of Shangri-La city range from 99°20′ E to 100°19′ E and from 26°52′ N to 28°52′ N, at the junction of Yunnan, Sichuan, and Tibet. The highest altitude is 5545 m above sea level, and the lowest is 1503 m (average elevation is 3459 m above sea level). The vegetation coverage reaches 89%, of which 59% is coniferous forest, 15.6% broad-leaved forest, 18% shrub, and 3.7% grassland and crop. The annual average temperature is 5.4 °C, with December being the coldest month in Shangri-La City. The average temperature in December is from −2 °C to 6 °C with an extreme minimum of −27.4 °C, and July is the hottest month with an average temperature from 12 °C to 14 °C and an extreme maximum temperature of 25.6 °C [48]. The average annual rainfall is from 268 mm to 945 mm, and the frost-free period is from 129 to 197 days [49]. The soil type is mainly dark brown forest soil [50].

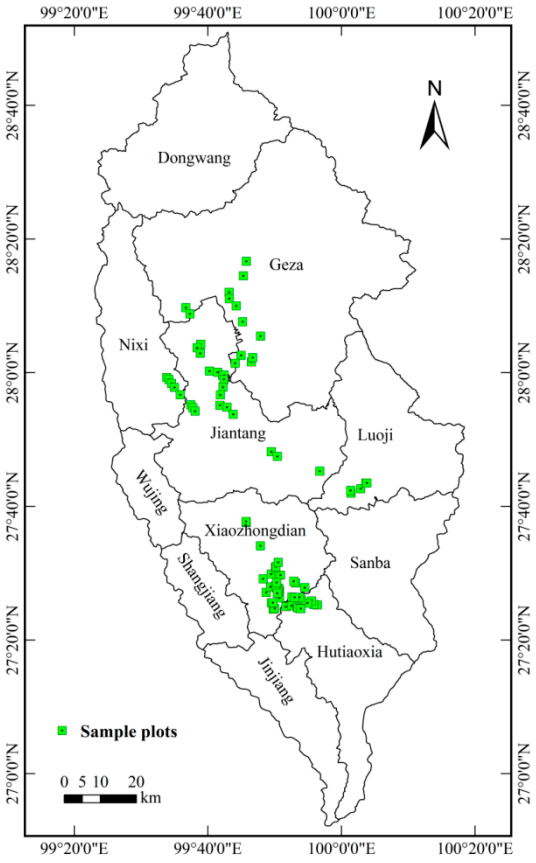


Figure 2. The location of study sites and the plots.

2.3. Data Investigation and Measurement

In August and September 2016, the biomass of 84 plots and 100 sampling trees were investigated and calculated, with the area per sample plot being 0.09 ha. We recorded each plot's location coordinates, elevation, slope degree, direction, and the measured DBH and *H* of each tree in the sample plots. Then we calculated the stand average tree height, average height of the dominant trees, average DBH, and the SD. Meanwhile, three standard trees with a similar average DBH and H in the plot were selected to determine the stand

age. Moreover, we measured the height of 3 to 6 dominant trees evenly distributed in the sample plot and used their average value as the mean dominant height [51]. The average heights of the dominant trees in the plots ranged from 3.60 to 29.00 m. The mean height of the stand was from 2.82 to 24.30 m, with their mean values being 12.59 and 10.36 m, respectively. The AGE ranged from 8 to 150 a, the stand density from 489 to 8500 trees·ha^{-1}, and the SV from 8.36 to 719.05 m^3 ha^{-1} (Table 1).

Table 1. The primary characteristics of the plots (n = 84). H_t is the average height of dominant trees in the stand, H_m is the mean height of the stand, D_g is the diameter corresponding with the mean basal area at breast height, AGE is the age of stand, SD is the stand density, and SV is the stand volume.

Variables		Minimum	Maximum	Mean	Standard Deviation
Stand	H_t (m)	3.60	29.00	12.59	4.70
	H_m (m)	2.82	24.30	10.36	4.13
	D_g (cm)	3.99	41.27	13.97	5.55
	AGE (a)	8	150	41	21
	SD (trees ha^{-1})	489	8500	2888	1541
	SV (m^3 ha^{-1})	8.36	719.05	229.40	133.88
Biomass	Wood (t ha^{-1})	2.87	236.19	76.30	44.67
	Bark (t ha^{-1})	0.51	28.24	10.65	6.18
	Needles (t ha^{-1})	6.23	70.98	33.23	10.95
	Branches (t ha^{-1})	1.51	23.00	6.17	2.55
	Above-ground (t ha^{-1})	11.12	344.38	126.35	60.45
	Roots (t ha^{-1})	0.80	31.47	10.87	5.29
	Total (t ha^{-1})	11.92	375.85	137.23	65.53
BEF	Wood	0.762	0.926	0.873	0.030
	Bark	0.074	0.238	0.127	0.030
	Needles	0.141	2.006	0.536	0.366
	Branches	0.022	0.482	0.106	0.090
	Above-ground	1.163	3.488	1.642	0.456
	Roots	0.080	0.257	0.140	0.036
	Total	1.265	3.707	1.782	0.486
BCEF	Wood	0.279	0.375	0.335	0.023
	Bark	0.030	0.092	0.048	0.010
	Needles	0.050	0.852	0.208	0.151
	Branches	0.008	0.205	0.041	0.037
	Above-ground	0.413	1.482	0.632	0.197
	Roots	0.032	0.099	0.055	0.014
	Total	0.449	1.575	0.686	0.210

The sample tree's length was measured after logging, and the DBH, H, and tree age were measured. In total, we harvested 100 sample trees, with the DBH ranging from 3.99 to 41.27 cm (mean of 13.97 cm), the tree height from 4.20 to 33.00 m (mean of 14.50 m), and the tree's age ranged from 18 to 258 a (mean of 60.17 a). The biomass per component ranged from 0.06 to 1652.72 kg (Table 2). Moreover, the biomass of the tree components was destructively measured, including wood, bark, branches, needles, and roots; stem diameters and bark thickness were recorded according to the stem height at 0, 0.5, 1.5, and 2.5 m to obtain the stem volume [39,40]. We measured the fresh weight of the wood and bark in 2 m segments. Then a sample disc, with about 4 cm thickness per segment, was sampled to obtain the moisture content and wood or bark density. We weighed the branches (fresh biomass) and needles in the field and sampled (at least 5% of their fresh mass) to assess dry weight. All samples were dried to a constant mass in the laboratory [52]. Regarding wood and bark, we calculated the dry mass using the disc's density and the corresponding volume per stem segment. For the branches and needles, we used the proportions of the total fresh masses and the moisture content of the samples [38].

Table 2. The primary characters of the sampling trees (n = 100). n is the number of trees, H is the tree height, DBH is the diameter at breast height, and age is the tree age.

Variables	Minimum	Maximum	Mean	Standard Deviation
n	100	100	100	-
H (m)	4.20	33.00	14.50	6.65
DBH (cm)	5.60	58.90	23.30	14.03
age (a)	18	258	60.17	45.08
Wood biomass (kg)	2.55	1088.25	191.55	270.71
Bark biomass (kg)	0.25	134.60	21.92	33.31
Needles biomass (kg)	0.06	34.84	6.41	7.26
Branches biomass (kg)	0.21	160.91	39.37	44.36
Above-ground biomass (kg)	4.03	1398.68	259.24	347.27
Roots biomass (kg)	1.51	275.38	51.90	66.47
Total biomass (kg)	5.54	1652.72	311.14	412.94

Moreover, according to the methodology guidelines from the IPCC [18], the BEF values of each component per plot were calculated using the proportions of the biomass of each component to the stem biomass. The BCEF values were calculated by the ratios of the biomass of each component to the stand volume for each biomass component (including wood, bark, needles, branches, roots, above-ground, and total biomass).

$$\mathrm{BEF}_i = B_i / B_{\mathrm{stem}} \quad (1)$$

$$\mathrm{BCEF}_i = B_i / \mathrm{SV} \quad (2)$$

where BEF_i is the BEF value of the i-th component, B_i is the biomass of the i-th component, B_{stem} is the stand stem biomass, BCEF_i is the BCEF value of the i-th component, and SV is the stand volume.

2.4. Model Fitting

Among the 84 sample plots, we randomly selected 63 for modeling, and the remaining 21 sample plots were used for testing. Among the 100 sample trees, 75 sample trees were randomly chosen for modeling, and the other 25 sample trees were used for testing. The power function was selected to construct the individual biomass static models [53,54], and the Richards, Logistic, Gompertz, Korf, and Weibull distributions were employed to model individual tree biomass growth and stand biomass, while BEFs and BCEFs changed with the stand age [51].

These models were constructed using the R statistical software [55]. The number of trees in the corresponding diameter classes was obtained, and then the percentage of the corresponding diameter classes and cumulative percentage of the diameter classes were calculated. The cumulative diameter structure of each plot was based on the Richards function, and the parameter prediction model was used to describe the dynamic change law of the stand diameter distribution. Finally, the nonlinear fitting method in the 1stOpt software [56] was used to find the optimal functional relationship between its parameters, the stand age, and the stand density index.

The biomass equations or growth models could be evaluated based on several statistical indicators. For instance, Zeng et al. [57,58] selected several indicators to assess the model's performance, with the coefficient of determination (R^2) and the root mean square error (RMSE) used as the essential indexes of model selection.

$$R^2 = 1 - \frac{\sum_{i=1}^{n} (y_i - \hat{y}_i)^2}{\sum_{i=1}^{n} (y_i - \overline{y})^2} \quad (3)$$

$$\mathrm{RMSE} = \sqrt{\frac{\sum_{i=1}^{n}(y_i - \hat{y}_i)^2}{n-1}} \quad (4)$$

$$\mathrm{EE} = \frac{1}{N}\sum_{i=1}^{N}\left(\frac{y_i - \hat{y}_i}{\hat{y}_i}\right) \times 100\% \quad (5)$$

$$\mathrm{RMA} = \frac{1}{\mathrm{N}}\sum_{i=1}^{N}\left|\frac{y_i - \hat{y}_i}{\hat{y}_i}\right| \times 100\% \quad (6)$$

where y_i is the observed value of y, $\hat{y}_i$ is the predicted value of y, $\overline{y}$ is the mean of y, n is the number of samples, and N is the sample size.

2.5. Method Evaluation

We chose two error indexes, the mean relative error (MRE) and the mean relative absolute error (MRAE), to evaluate the estimation performance of five methods using different stand components. All statistical indicators utilizes the SPSS software [59].

$$\mathrm{MRE} = \frac{1}{n}\sum\left(\frac{yi - \hat{y}_i}{\hat{y}_i}\right) \times 100\% \quad (7)$$

$$\mathrm{MRAE} = \frac{1}{n}\sum\left|\frac{y_i - \hat{y}_i}{\hat{y}_i}\right| \times 100\% \quad (8)$$

where y_i is the observed value of the response variable, $\hat{y}_i$ is the predicted value of the response variable, and n is the sample size of the validation data.

3. Results

3.1. Model Evaluation

3.1.1. Stand Biomass of Different Components (SBA)

The stand biomass growth models (SBA) were built using the independent variable of stand age to estimate the stand biomass growth for the different components according to

$$SB_i = f(t) \quad (9)$$

where SB_i is the stand biomass per component and t is the stand age, while the functions are the Richards, Logistic, Gompertz, Korf, and Weibull.

Due to the highest R^2 and lowest RMSE per component, the logistic function was selected to fit the growth of the wood, roots, and the above-ground biomass, the Korf function was employed to fit the growth of bark biomass, and the Richards function to fit the growth of the branches and needles biomass. All models and their estimation results are reported in Table 3.

Table 3. The estimation result of the SBA. W is the biomass of each component (wood, bark, needles, and branches), above-ground, and roots biomass of the stand. N is the stand density, and AGE is the stand age.

Components	Model Forms	Fitting			Test		
		n	R^2	RMSE	n	EE	RMA
Wood	$W = \frac{112.24}{1 + \exp\left(4.32 - 0.113 \times \left(\frac{N}{1000}\right)^{0.188} \times \mathrm{AGE}\right)}$	63	0.655	24.198	21	30.628	45.761
Bark	$W = 24.607 \times \exp\left(-83.459 \times \left(\frac{N}{1000}\right)^{-0.011} \times \mathrm{AGE}^{-1.259}\right)$	63	0.583	4.066	21	16.749	37.444
Needles	$W = 5.161 \times \left(\frac{1-\exp\left(-0.345 \times \left(\frac{N}{1000}\right)^{-0.942} \times \mathrm{AGE}\right)}{1-\exp\left(-0.345 \times \left(\frac{N}{1000}\right)^{-0.942} \times 20\right)}\right)^{2.782}$	63	0.401	1.383	21	24.327	32.101

Table 3. *Cont.*

Components	Model Forms	Fitting			Test		
		n	***R*²**	**RMSE**	***n***	**EE**	**RMA**
Branches	$W = 23.987 \times \left(\frac{1-\exp\left(-0.185\times\left(\frac{N}{1000}\right)^{-0.647}\times \mathrm{AGE}\right)}{1-\exp\left(-0.185\times\left(\frac{N}{1000}\right)^{-0.647}\times 20\right)} \right)^{3.209}$	63	0.497	7.788	21	16.124	25.024
Above-ground	$W = \frac{173.25}{1+\exp\left(3.281-0.093\times\left(\frac{N}{1000}\right)^{0.217}\times \mathrm{AGE}\right)}$	63	0.611	34.849	21	23.393	34.989
Roots	$W = \frac{30.514}{1+\exp\left(3.626-0.141\times\left(\frac{N}{1000}\right)^{0.05}\times \mathrm{AGE}\right)}$	63	0.561	6.849	21	20.008	31.577

The R^2 ranged from 0.401 to 0.655, with the corresponding value for the wood biomass being the highest and the needles being the lowest. However, the needles had the smallest RMSE (1.383). The average relative error (EE) ranged from 16.749 to 30.628, all positive, indicating that the equation estimation was on the high side, and the absolute mean relative error (RMA) was above 32.101 (Table 3).

3.1.2. Stand Stem Biomass Combined with Biomass Expansion Factors (SB+BEF)

Based on the growth relationship of the stand stem biomass (SB_{stem}) and biomass expansion factors (BEF_i) with stand age (t), the stand biomass of the different components at a certain age was predicted using the product of SB_{stem} and the corresponding BEF values. The corresponding equation is presented in Equation (10), revealing that the stand biomass growth can be estimated by combining the stand stem biomass with biomass expansion factors (SB+BEF).

$$\begin{cases} SB_{stem} = f(t) \\ BEF_i = f(t) \\ SB_i = SB_{stem} \cdot BEF_i \end{cases} \quad (10)$$

where SB_{stem} is the stand stem biomass, BEF_i is the biomass expansion factor, SB_i is the stand biomass per component, and t is the stand age. The functions are logistic, linear, power, and logarithm.

The logistic function was selected to fit the stem's growth, and the linear function fitted the growth of wood, bark, needles, and above-ground. The power function fitted the growth of the branches, and the logarithm function was selected to fit the growth of the roots. All models and the estimated results are reported in Table 4.

Table 4. The estimation result of the SB+BEF. SB_{stem} is the stem biomass, N is the stand density, AGE is the stand age, y is the biomass expansion factors of each component (wood, bark, needles, branches), and above-ground and roots biomass expansion factors.

Variables		Model Forms	Fitting			Test		
			n	***R*²**	**RMSE**	***n***	**EE**	**RMA**
Stem biomass		$SB_{stem} = \frac{155.663}{1+\exp\left(4.946-0.107\times\left(\frac{N}{1000}\right)^{0.288}\times \mathrm{AGE}\right)}$	63	0.625	36.803	21	33.550	49.434
BEF	Wood	$y = 0.875 - 0.0000979 \times \mathrm{AGE}$	63	0.006	0.032	21	0.590	2.532
	Bark	$y = 0.125 + 0.0000979 \times \mathrm{AGE}$	63	0.006	0.032	21	−3.882	17.008
	Needles	$y = 4.42/\mathrm{AGE} - 0.024$	63	0.674	0.058	21	−13.500	30.082
	Branches	$y = 16.069 \times \mathrm{AGE}^{-0.959}$	63	0.700	0.224	21	−17.071	24.432
	Above-ground	$y = 22.546/\mathrm{AGE} - 0.979$	63	0.694	0.282	21	−5.721	8.774
	Roots	$y = 0.936 - 0.168 \times \ln(\mathrm{AGE})$	63	0.515	0.087	21	−5.129	14.425

In the biomass growth equation constructed by biomass expansion factors (BEF), the effect of wood and bark was not ideal, with R^2 = 0.006 but RMSE = 0.032, which was the smallest. Except for the wood biomass, the mean relative errors of the other components

(bark, needles, branches, above-ground, and roots) were all negative, and RMA ranged from 2.532 to 30.082 (Table 4).

3.1.3. Stand Volume Combined with Biomass Conversion and Expansion Factors (SV+BCEF)

By modeling the relationship of the stand volume (SV) and the BCEFs of each component with stand age, the stand biomass of the different components at a certain age could be predicted using the product of SV and the corresponding BCEF values. The stand biomass growth was estimated using the method of stand volume combined with the biomass conversion and expansion factors (SV+BCEF) using the equation below:

$$\begin{cases} \mathrm{SV} = f(t) \\ \mathrm{BCEF}_i = f(t) \\ \mathrm{SB}_i = \mathrm{SV} \cdot \mathrm{BCEF}_i \end{cases} \quad (11)$$

where SV is the stand volume, BCEF_i is the biomass conversion and expansion factors, SB_i is the stand biomass of each component, and t is the stand age. The functions are logistic, linear, power, and logarithm.

The logistic function was selected to fit the stand volume growth, the linear function to fit the growth of wood, bark, needles, and branches, the power function to fit the above-ground growth, and the logarithm function was selected to fit the growth of roots. All models and their estimation results are reported in Table 5.

Table 5. The estimation result of the SV+BCEF. SV is the stand volume, N is the stand density, AGE is the stand age, y is the biomass conversion and expansion factors of each component (wood, bark, needles, branches), and above-ground and roots biomass conversion and expansion factors.

Variables		Model Forms	Fitting			Test		
			n	R^2	RMSE	n	EE	RMA
Stand volume		$\mathrm{SV} = \frac{404.278}{1 + \exp\left(4.887 - 0.113 \times \left(\frac{N}{1000}\right)^{0.236} \times \mathrm{AGE}\right)}$	63	0.647	92.297	21	32.339	47.855
BCEF	Wood	$y = -0.00037 \times \mathrm{AGE} + 0.351$	63	0.151	0.024	21	−1.540	4.339
	Bark	$y = \exp(-3.07 + 2.011/\mathrm{AGE})$	63	0.031	0.011	21	−4.923	15.257
	Needles	$y = -0.012 + 1.827/\mathrm{AGE}$	63	0.683	0.023	21	−15.428	30.720
	Branches	$y = -0.013 + 7.531/\mathrm{AGE}$	63	0.705	0.092	21	−16.154	24.151
	Above-ground	$y = 4.294 \times \mathrm{AGE}^{-0.535}$	63	0.712	0.119	21	−6.610	11.013
	Roots	$y = 0.387 - 0.072 \times \ln(\mathrm{AGE})$	63	0.593	0.032	21	−6.670	14.019

In the biomass growth equation constructed by BCEF, the R^2 of wood and bark were small, 0.151 and 0.031, respectively, and the mean relative errors of the five components were all negative, indicating that the estimation of each equation was generally low. The RMA of wood as the smallest at 4.339 (Table 5).

3.1.4. Individual Biomass Static Models Combined with Stand Diameter Structure (IB+SDS)

For the static biomass models of the components, we used the power function as the primary form of the model to construct the *Pinus densata* individual tree biomass model. We built the *Pinus densata* individual tree biomass model based on the tree height and diameter at breast height as the independent variables of each dimension of the biomass model. Moreover, the height curves were fitted to obtain the tree height corresponding with the DBH classes. The basic models were also selected as the power function, logistic equation, Korf equation, and Richards equation. The one presenting the best fitting and prediction accuracy performance was used further.

The stand biomass growth was estimated by using the individual biomass static model combined with the stand diameter structure (IB+SDS):

$$\begin{cases} \mathrm{IB}_i = \mathrm{f}(\mathrm{DBH}, H), \text{ and } H = \mathrm{f}(\mathrm{DBH}) \\ \mathrm{PDF}(\mathrm{DBH}) = \mathrm{f}(\mathrm{DBH}) \\ p = f(\mathrm{AGE}, \mathrm{SD}) \\ \mathrm{SB}_i = \sum N \cdot p_j \cdot \mathrm{IB}_{i,j} \end{cases} \quad (12)$$

where IB_i is the individual biomass, and the basic function considers using four power function models. The independent variables are DBH, H, and $\mathrm{DBH}^2\mathrm{H}$ (pseudo volume). DBH is the diameter at breast height, H is the tree height, AGE is the stand age, SD is the stand density, N is the cumulative probability of the diameter classes from minimum class, p_j is the estimation of the cumulative probability distribution functions for fitting the stand diameter structure, and SB_i is the stand biomass of each component. The functions of the tree height curve are logistic, power, Bates, Wykoff, and Richards.

For the stand diameter structure models, we used the Richards function (Equation (13)), fitting the cumulative percentage along with the diameter classes per plot. Table 6 reports the fitting results with the R^2 values of all plots exceeding 0.9, indicating an excellent fitting effect that better reflected the actual situation of a stand diameter accumulation distribution (Table 6). Then, the estimation parameters b and c were estimated utilizing the stand age and stand density, thus predicting the diameter class distribution at a specific time.

$$y = (1 - \exp(b \cdot R_d))^c \quad (13)$$

where y is the cumulative percentage of the stand's diameter classes, R_d is the diameter class (cm), and b and c are the parameters to be estimated.

Table 6. The statistics of the estimation parameters of the cumulative distribution function of the stand diameter structure for all plots.

Parameters	Minimum	Maximum	Mean	Standard Deviation
b	0.044	1.579	0.326	0.275
c	1.307	402.311	26.425	60.700
R^2	0.905	1.000	0.977	0.018
RMSE	0.118	0.896	0.427	0.180

Finally, the total biomass per diameter class is obtained from the tree number with different diameter classes and the corresponding component biomass. Then, the biomass of all trees for each component or the total stand biomass is obtained by adding all diameter classes.

For each component, the static biomass growth model of an individual tree was estimated by a power function equation, with models and estimation results listed in Table 7.

As reported in Table 7, the R^2 of the biomass growth model per component of the wood was appealing, but the R^2 of the needles as 0.674, lower than the other components. The mean relative errors (EE) of each component were all negative, indicating that the error estimating each equation was generally low. The EE of the parameters (b, c) was also negative (Table 7).

Table 7. The estimation result of the IB+SDS. IB is the individual tree biomass of each component (wood, bark, needles, branches), above-ground, and root individual tree biomass. DBH is the diameter at breast height, H is the value corresponding to DBH on the tree height curve, b and c are the stand diameter structure parameters, x_1 represents the AGE of the stand age, and x_2 represents the stand density.

Variables		Model Forms	Fitting			Test		
			n	R^2	RMSE	*n*	EE	RMA
Individual tree biomass	Wood	$IB = 0.030 \times DBH^{1.746} \times H^{1.021}$	75	0.990	28.921	25	−2.701	12.067
	Bark	$IB = 0.0034 \times DBH^{1.222} \times H^{1.640}$	75	0.898	11.175	25	−9.796	31.204
	Needles	$IB = 0.045 \times DBH^{2.498} \times H^{-1.143}$	75	0.674	4.389	25	13.115	41.071
	Branches	$IB = 0.170 \times DBH^{2.007} \times H^{-0.386}$	75	0.831	18.989	25	−18.635	42.069
	Above-ground	$IB = 0.075 \times DBH^{1.700} \times H^{0.875}$	75	0.990	36.145	25	−5.802	15.163
	Roots	$IB = 0.025 \times DBH^{2.221} \times H^{0.082}$	75	0.999	2.495	25	−2.357	6.368
Tree height curve		$H = \frac{41.133}{1 + 5.809 \exp(-0.048 \times DBH)}$	75	0.877	2.349	25	−1.511	15.523
Stand diameters structure parameters	b	$b = (-122275 - 4884.247 \cdot x_1 + 337.997 \cdot x_2 - 53.09 \cdot {x_1}^2 - 0.109 \cdot {x_2}^2 + 6.29 \cdot x_1 \cdot x_2)/(1 - 18670.28 \cdot x_1 + 86.892 \cdot x_2 - 541.006 \cdot {x_1}^2 - 0.426 \cdot {x_2}^2 + 56.942 \cdot x_1 \cdot x_2)$	63	0.883	0.105	21	−4.029	27.853
	c	$c = 21.949 - 0.0026 \cdot x_2 + 478.319 \cdot \exp(-\exp(-(x_1 - 14.209)/-1.378) - (x_1 - 14.209)/-1.378 + 1)$	63	0.874	25.203	21	−40.692	51.911

3.1.5. Individual Biomass Growth Models Combined with Stand Density (IB+SD)

The individual biomass growth models combined with the stand density (IB+SD) can predict the stand biomass growth. The individual tree biomass growth model per component is constructed, and the product of the individual biomass and stand density is calculated to obtain the components' stand biomass at a specific time (Equation (14)). The stand density of each plot is assumed not to change with the stand growth.

$$\begin{cases} IB_i = f(t) \\ SB_i = N \cdot IB_i \end{cases} \quad (14)$$

where IB_i is the individual biomass, t is the stand age, N is the stand density, and SB_i is the stand biomass of each component. The functions employed for the IB_i are Richards, Logistic, and Korf.

The Richards function was selected to fit the growth of the wood, needles, branches, and roots biomass, and the logistic function fitted the bark biomass growth. The Korf function was selected to fit the growth of the above-ground biomass. The models and the corresponding estimation results are reported in Table 8.

Table 8. The estimation result of the IB+SD. The IB is the individual tree biomass of each component (wood, bark, needles, branches), above-ground, and root tree biomass. The age is the tree age.

Variables		Model Forms	Fitting			Test		
			n	R^2	RMSE	*n*	EE	RMA
Individual tree biomass	Wood	$IB = 1378 \times (1 - \exp(-0.0111 \times age))^{2.880}$	75	0.889	92.088	25	−19.700	46.527
	Bark	$IB = \frac{92.881}{1 + \exp(4.87 - 0.057 \times age)}$	75	0.801	15.622	25	−16.904	50.969
	Needles	$IB = 17.262 \times (1 - \exp(-0.03 \times age))^{3.743}$	75	0.454	5.684	25	−27.905	53.246
	Branches	$IB = 131.534 \times (1 - \exp(-0.025 \times age))^{3.96}$	75	0.733	23.870	25	−16.730	57.181
	Above-ground	$IB = 1291.748 \times \exp(-5.876 \times \exp(-0.021 \times age))$	75	0.892	121.085	25	−22.067	44.151
	Roots	$IB = 253.572 \times (1 - \exp(-0.015 \times age))^{3.105}$	75	0.855	26.296	25	−16.212	53.203

The best individual tree biomass growth model for the different components is listed in Table 8, where the R^2 of all models exceeded 0.45. Specifically, wood, bark, above-ground, and roots attained a value greater than 0.8, and the needles presented the lowest value of 0.454. The mean relative errors of each component were all negative.

3.2. Method Comparison

The MRE and MRAE were used to evaluate the error of all five methods. As illustrated in Figure 3, the MRE values of both SB+BEF and SV+BCEF for all components were not significantly different from zero (except for the wood biomass estimated by the SB+BEF method and the total biomass by the SV+BCEF method). In both the SBA and IB+SD methods, the MRE values were extremely significant to zero. However, for the IB+SDS, the difference's significance varied depending on the biomass component, with the MRE of the roots and the total stand biomass significantly different to zero. However, the other components' differences between MRE and zero were insignificant. Moreover, among the five methods, the MRE of the biomass (each component, above-ground, roots, total biomass) estimated by the SBA method was significantly larger than that of the IB+SD method. For the MRE of the wood biomass, the biomass estimated by SBA, SB+BEF, and SV+BCEF was significantly different from the one calculated by IB+SDS and IB+SD. The significance of the mean relative error of the above-ground, roots, and total biomass is depicted in the Figure 3.

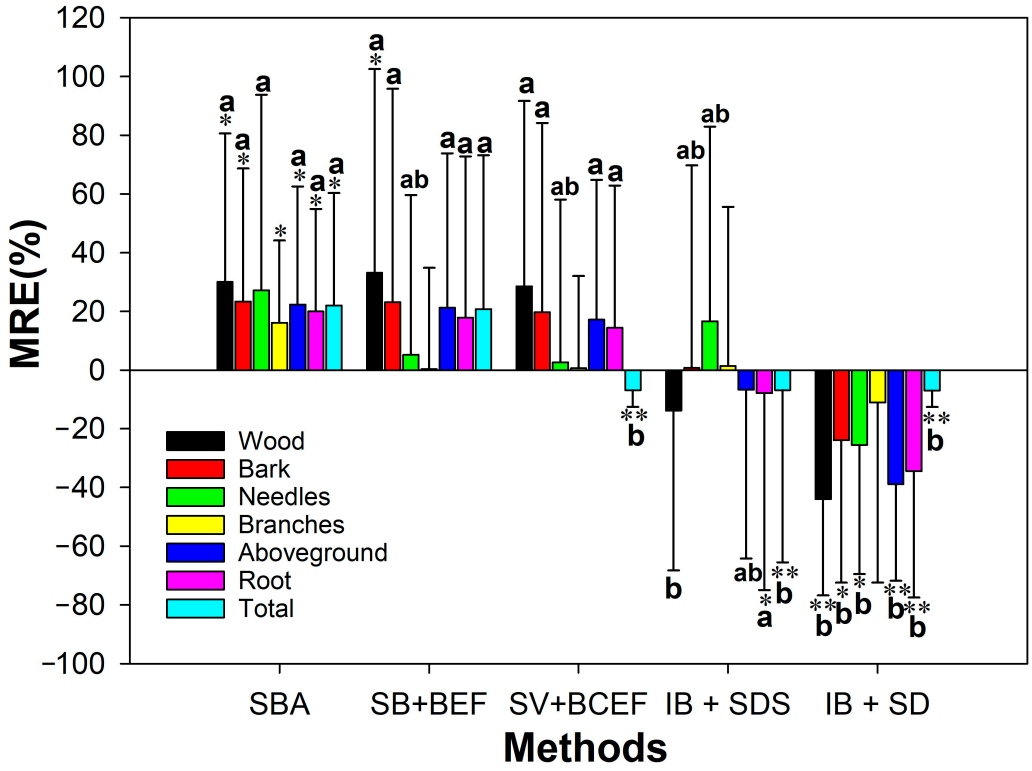


Figure 3. Mean relative error (MRE) of five methods for the different components. The statistical test results of the significant differences of MREs from zero: * and ** represent the significance levels of 0.05 and 0.01, respectively. The letters a, ab, and b indicate the significance of the same component between different methods at the significance levels of 0.05.

In addition, for the IB+SD method, the value of the MRE of the different components ranged from −44.044 to −7.019%, the value of the total biomass is the lowest, and the MRE value is −7.019%. The biomass MRE using the SV+BCEF method was positive, except for the total biomass. The MRE ranged from −6.914 to 28.582%. Regarding IB+SDS, the MRE ranged from −13.84 to 16.649%, while the MRE of each biomass component estimated by the SBA method and the SB+BEF method ranged from 16.124 to 30.087% for the SBA

method. The MRE range was 0.397 to 33.183% for the SB+BEF method. The MRE values were all positive, indicating that the biomass estimated by these two methods was smaller than the measured value.

Compared with MRE, MRAE reflected the absolute bias between the observed and predicted values, and there was no offset between positive and negative. As depicted in Figure 4, except for the significant difference between the MRAE of needles, biomass estimated by the SBA method, and zero, the MRAE of the remaining components (wood, bark, branches, roots), above-ground, and total biomass was significantly different from zero. For the MRAE of branch biomass, the MRAE of biomass estimated by the IB+SD method was significantly larger than the MRAE of the biomass estimated by the remaining three methods (SBA, SB+BEF, and SV+BCEF) except for the IB+SDS method. For the total biomass, the MRAE of the biomass estimated using SBA and SB+BEF was significantly larger than that estimated using the other three methods (SV+BCEF, IB+SDS, and IB+SD).

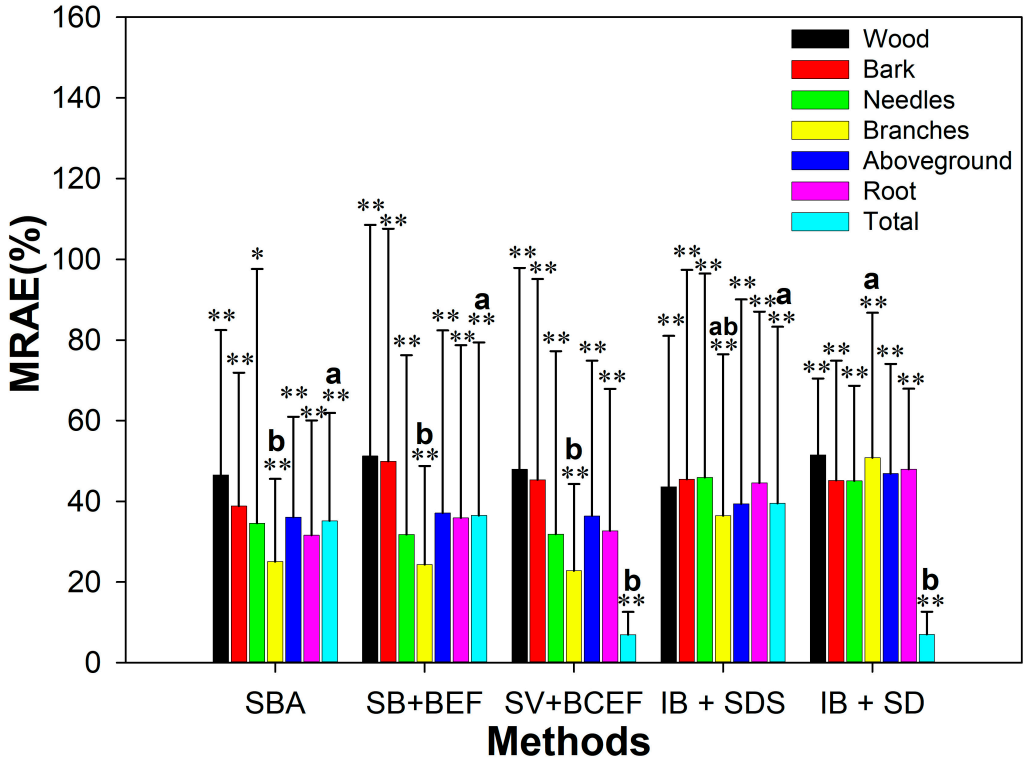


Figure 4. Mean relative absolute error (MRAE) of five methods for the different components. The statistical test results of the significant differences of MRAEs from zero: * and ** represent the significance levels of 0.05 and 0.01, respectively. The letters a, ab, and b indicate the significance of the same component between different methods at the significance levels of 0.05.

Among the biomass components estimated by the five methods, the MRAE values of the wood biomass were all larger (except for the needles biomass, which had the largest MRAE value of the IB+SDS method). The SV+BCEF and IB+SD methods had the lowest MRAE values for the estimated total biomass, and the branches had the lowest MRAE values estimated by the other three methods.

4. Discussion

4.1. Estimation Comparison

This study used five methods to calculate the above-ground biomass, roots biomass, and biomass of different components of the *Pinus densata*. For the calculations, we used the measured sample plot data of *Pinus densata* and simulated the dynamic growth model system of the *Pinus densata* biomass. The model system reflected the effects of stand density, DBH, stand volume, and biomass factors on biomass. Overall, this study's results revealed

that the stem biomass combined with the biomass expansion factors (BEF) method, the stand volume combined with the biomass conversion and expansion factors (BCEF) method, and the method of combining individual tree biomass with the stand diameter structure presented less errors and a higher prediction accuracy. The stand biomass was related to the biomass expansion factors, stand volume, biomass conversion, expansion factor, and stand diameter structure [60–62]. Moreover, the stand biomass was related to the stand volume, while introducing the stand volume as a variable to calculate the biomass reduced the model's uncertainty [11]. Therefore, many models have been established to derive biomass from the stand volume [10,63], significantly affecting the stand biomass. These findings were consistent with the conclusions of Zeng et al. [64], Dong et al. [21], and Jagodziński et al. [16,39,40] on biomass and accumulation of *Larix decidua* Mill., *Abies alba* Mill., *Pinus sylvestris* L.

Jagodziński et al. [38] researched Scots pine, and Usoltsev et al. [65] concluded that biomass expansion and conversion were related to the stand age, confirming this study's rationality and the feasibility using age as a variable to predict biomass growth. The change in BEF in response to the changing relationships of stem volume and biomass to total tree volume and biomass with the increasing stand age was an essential consideration in biomass estimates [66]. In this study, BEF, BCEF, and stand age presented a certain regularity, as BEF and BCEF decreased with the increase of stand age until reaching a constant value [67,68]. Similar to Jagodziński et al. [38,69], who studied young birch (*Betula pendula*) and young Scots pine stands, the changes of the BEF and BCEF with the stand age conformed to the biological law of tree growth biomass changes, i.e., the biomass changed with the growth of the trees after reaching a certain age, after which the biomass saturated. For that reason, the biomass of young tree stands cannot be calculated using the BCEF derived for older tree stands [69,70]. This study avoided this issue because we modeled the variations of BEF and BCEF with stand age. Because the stand volume and stand diameter structure (SDS) were directly related to stand factors such as diameter at breast height and tree height, which were directly related to tree growth, they directly affected the stand biomass and carbon storage [71,72]. In addition, the growth change of stem biomass with age was also significantly correlated with DBH and tree height, so the growth of stem biomass was also in line with the biological changes in tree growth.

In this study, among the biomass growth equations constructed using two methods, SB+BEF and SV+BCEF, the models for BEF and BCEF were constructed using stand age as the independent variable. The R^2 values of the constructed equations of BEF and BCEF for wood (R^2 = 0.006 in Table 4 and R^2 = 0.151 in Table 5) and bark (R^2 = 0.006 in Table 4 and R^2 =0.031 in Table 5) were all low. Lehtonen et al. [68] used stand age as the independent variable to construct some BEF models. For Norway spruce stands, the R^2 of BEF models ranged from 0.2020 to 0.3622, and the values for the broadleaved stands ranged from 0.0377 to 0.2399; then, they suggested applying the constant as the R^2 was lower than 0.25. Therefore, the proportions of wood and bark to the stem were relatively constant, and the constant BEF values should be used in specific situations, particularly when estimating bark and wood biomass [69]. Moreover, the SBA and IB+SD methods predicted biomass growth in model construction, as these two methods were closely related to stand density. Trees' biological characteristics and biomass allocation patterns change with the stand growth, and these changes may be related to the tree size increases with age and changes in stand density [73]. The stand density significantly changes the vertical and horizontal stand structure and stand density can dramatically affect the growth and development of stands. The increase in stand density leads to intensified competition among trees, resulting in intensified intra-specific and inter-specific competition in its upper and lower parts, thereby changing biomass allocation [38,61,74].

4.2. Applicability Analysis of the Estimation Methods

The five stand biomass estimation methods are logically equivalent [46]. And the equivalence between the five methods means that differences between methods may arise

from random or non-random processes associated with sampling and modeling [75]. In this study, considering the destructiveness of forest biomass investigation, the clear-cutting method was not used to measure the trees in the sample plot, only the biomass of the standard tree was measured. And the measurement methods used are consistent. Furthermore, the sampling range of both tree and plot covers the tree or stand age, stand density, and tree size of *Pinus densata* in the study area (Tables 1 and 2). Thus, the equivalence between the five methods meant that the differences between methods may be due to the process related to modeling. The individual tree, whole stand, and the diameter distribution models were used, and they had advantages and disadvantages [51,75]. The whole stand models provided better estimates at the stand level, but such estimation results lacked stand structure information [41]. It is well known that building models from the individual tree level to the whole stand level to estimate biomass can lead to inaccurate estimation results due to accumulated errors [45,46]. However, there is a lack of research on the specific error size. This study quantified the errors from the individual tree level to the stand level, and the errors in estimating the biomass of each component using different methods were compared.

Moreover, the biomass growth estimation system of *Pinus densata* forests was constructed based on individual tree, stand diameter structure, and stand data. Each method applied to different conditions. The IB+SDS and IB+SD methods calculated the stand biomass of *Pinus densata* by calculating the biomass of an individual tree and then combining the corresponding stand factors to calculate the stand biomass of *Pinus densata*. Using the individual tree biomass model as the base model to estimate, the stand biomass growth could better describe the stand [41,45,47,76]. Stand density is an essential factor affecting the growth and productivity of stand [11].

The consideration of constant stand density is based on the method's applicability. Because the *Pinus densata* stands in this study were relatively homogeneous and the hectare values of the trees (trees ha^{-1}) was used as the stand density, the IB+SD method was suitable for estimating the biomass of plantations with a consistent stand age. When the stand structure is relatively complex, the introduction of the stand diameter structure can better fit the equation to accurately estimate biomass, so in this case, the IB+SDS method was more suitable for estimating *Pinus densata* stand biomass. Generally, the distribution of trees on the stand is relatively uniform in a plantation, and the hectare values of the trees and the average size of the stand are frequently used as indicators of stand density, but stand density changes with the stand age or tree size [51]. The stand density index (SDI), proposed by Reineke, applies to plantations or a pure forest of the same age with a substantially similar management history [77]. In this study, the stand density was assumed not to change with the stand growth in the estimation IB+SD and IB+SDS method. The fixed stand density may bring errors in biomass estimation, but the standard DBH is required for the SDI, and the value is not uniform [51]. The usual value in Chinese forestry is 20 cm [51,78], but Reineke defines it as 25.4 cm [77], and Jiang et al. used a value of 12 cm in their study on Masson Pine [79]. Moreover, the stand self-thinning slope varies with tree species and geographical area. The slope value in Reineke's study was −1.605, which is a fixed value for most tree species. Luis et al. [80] used a slope value of −1.897. Zhang et al. [81] studied the self-thinning slope of fir and showed that the model with climate-sensitivity performed best. No specific value was given for the self-thinning slope of *Pinus densata*. Thus, the inappropriate standard DBH and stand self-thinning slope may cause more significant errors [51]. Furthermore, the spatial pattern of trees in natural forests is not homogeneous, which may make the relationship between diameter at breast height and stand density unstable [51]. Thus, the use of the stand density index may produce unexpected results. Using the stand density for natural forests should be appropriate.

The SBA, SB+BEF, and SV+BCEF estimation methods were the model constructed at the stand level. For the SBA method, each stand component calculated the stand biomass growth. Therefore, the SBA method is suitable for plantations or forests of the same age, where the stand age is relatively easy to obtain. It is more suitable to calculate the biomass

growth by points; the SB+BEF method is suitable for the biomass conversion factor when only tree trunk data can be obtained or is easy to obtain in the sample plot. The SV+BCEF method is suitable for stands whose stand volume is easy to measure, the stand biomass can be calculated by combining the stand volume with the biomass conversion expansion factor.

Although many remote sensing methods have been used to measure forest biomass, remote sensing observations still need to be combined with ground survey data [78]. Within a specific accuracy range, the research method in this paper can meet ground surveys. In addition, the remote sensing method can only observe the above-ground biomass. It cannot measure the root biomass of the forest. However, the roots biomass is also an essential part of the forest biomass [9], so the research in this paper can be used in future work—methods combined with remote sensing methods to conduct ground surveys.

Moreover, some research showed that the error estimates in an extended factor model of biomass constructed with age as the independent variable and that the error range was species-dependent [75]. Thus, this study included five estimations with age as the independent variable. Moreover, it is feasible to use age as a variable to predict forest biomass growth, and many scholars have also conducted related explorations in previous studies. Zavitkovski [82] showed that age significantly affected the relationship between above-ground roots, the biomass of above-ground components, and tree size. Introducing stand age as an auxiliary variable into the model with a diameter at breast height, diameter at breast height, and tree height as independent variables can improve the estimation effect of the model and reduce the error in the allometric growth equation of the above-ground components [80]. The biomass growth model with age has a higher fitting accuracy than the growth model without age as a variable [83]. Peichl et al. [66] studied the allometric growth and distribution of above-ground and roots tree biomass of four age sequences of white pine. They considered that age affects the distribution of biomass of each standing tree component during the growth process. This was related to comparing the biomass model without introducing the age factor. The introduction of the age variable can reduce the error of biomass estimation of wood samples of different ages. Xue et al. [84] established an individual tree biomass growth model for three tree species with standing tree age as an independent variable, indicating that the proportion of above-ground biomass in the standing tree growth cycle increased with age and constantly changed. Constructing a biomass growth model including stand age can realize biomass estimation on a regional scale at a specific time, which can be used for regional-scale biomass and carbon storage estimation and carbon sink potential assessment [85]. This study used stand age as a variable to construct a biomass growth equation, which provided models and methods for estimating the biomass and carbon storage of *Pinus densata* forests in Shangri-La.

5. Conclusions

This study provided a comprehensive overview of methods for estimating *Pinus densata* stand biomass in Shangri-La City in southwest China. Five methods for estimating biomass growth were established and evaluated, and the most suitable methods for estimating the biomass of different components of *Pinus densata* forests were screened out. These methods have certain biological rationality and accuracy: the stand stem biomass combined with BEF, the stand volume (SV) combined with BCEF, and the individual tree biomass combined with the change of stand diameter structure (SDS). Overall, these three methods showed good accuracy in estimating the total stand biomass, above-ground biomass, roots biomass, and biomass of different components of *Pinus densata* forests in this area.

However, choosing a method depends on the data available. As the stem data is easy to obtain and the biomass of other components is not easy to obtain, the stem biomass can be calculated. By constructing the allometric growth equation of BEF, the stem biomass combined with BEF can calculate the change of the different components with age. If stand volume data is not easy to obtain, the change in biomass of different components with age can be predicted by constructing the allometric equation of stand volume and combining it with the BCEF value. If the biomass of an individual tree is easy to obtain, the change of

forest biomass with age can be predicted using the biomass of an individual tree combined with the stand diameter structure. Overall, this work has a significant reference value for the growth estimation of stand biomass in afforestation and reforestation.

Author Contributions: G.C. participated in the collection of field data, conducted data analysis, and wrote the draft of the paper; X.Z. and C.L. (Chunxiao Liuand) participated in the collection of field data and data analysis; C.L. (Chang Liu) and H.X. helped with data analysis and writing of the paper. G.O. supervised and coordinated the research project, designed the experiment, and revised the paper. All authors have read and agreed to the published version of the manuscript.

Funding: The study was financially supported by the National Natural Science Foundation of China (grant numbers 31560209 and 31760206) and the Ten-Thousand Talents Program of Yunnan Province, China (YNWR-QNBJ-2018-184).

Acknowledgments: The authors would like to thank the faculty and students at the College of Forestry, Southwest Forestry University (SWFU), China, who provided and collected the data for this study. The authors would like to thank EditSprings (https://www.editsprings.cn) for the expert linguistic services.

Conflicts of Interest: The authors declare that they have no known competing financial interests or personal relationships that could have appeared to influence the work reported in this paper.

References

1. Six, J.; Callewaert, P.; Lenders, S.; De Gryze, S.; Morris, S.J.; Gregorich, E.G.; Paustian, K. Measuring and understanding carbon storage in afforested soils by physical fractionation. *Soil Sci. Soc. Am. J.* **2002**, *66*, 1981–1987. [CrossRef]
2. Pan, Y.; Birdsey, R.A.; Fang, J.; Houghton, R.; Kauppi, P.E.; Kurz, W.A.; Hayes, D. A large and persistent carbon sink in the world's forests. *Science* **2011**, *333*, 988–993. [CrossRef]
3. Alberdi, I.; Cañellas, I.; Bombín, R.V. The Spanish National Forest Inventory: History, development, challenges, and perspectives. *Pesqui. Florest. Bras.* **2017**, *37*, 361–368. [CrossRef]
4. Shuyong, L.; Shenggong, L.; Mei, H. Effects of thinning intensity on carbon stocks and changes in larch forests in China northeast forest region. *J. Resour. Ecol.* **2017**, *8*, 538–544. [CrossRef]
5. Augusto, L.; Boča, A. Tree functional traits, forest biomass, and tree species diversity interact with site properties to drive forest soil carbon. *Nat. Commun.* **2022**, *13*, 1097. [CrossRef]
6. Vogt, K. Carbon budgets of temperate forest ecosystems. *Tree Physiol.* **1991**, *9*, 69–86. [CrossRef]
7. Kurz, W.A.; Beukema, S.J.; Apps, M.J. Estimation of root biomass and dynamics for the carbon budget model of the Canadian forest sector. *Can. J. For. Res.* **1996**, *26*, 1973–1979. [CrossRef]
8. Brown, S. Measuring carbon in forests: Current status and future challenges. *Environ. Pollut.* **2002**, *116*, 363–372. [CrossRef]
9. West, P.W. *Tree and Forest Measurement*; Springer: Berlin/Heidelberg, Germany, 2015.
10. Castedo-Dorado, F.; Gómez-García, E.; Diéguez-Aranda, U.; Barrio-Anta, M.; Crecente-Campo, F. Aboveground stand-level biomass estimation: A comparison of two methods for major forest species in northwest Spain. *Ann. For. Sci.* **2012**, *69*, 735–746. [CrossRef]
11. He, X.; Lei, X.; Dong, L. How large is the difference in large-scale forest biomass estimations based on new climate-modified stand biomass models? *Ecol. Indic.* **2021**, *126*, 107569. [CrossRef]
12. Somogyi, Z.; Cienciala, E.; Mäkipää, R.; Muukkonen, P.; Lehtonen, A.; Weiss, P. Indirect methods of large-scale forest biomass estimation. *Eur. J. For. Res.* **2007**, *126*, 197–207. [CrossRef]
13. Li, H.; Lei, Y.; Zeng, W. Forest carbon storage in China estimated using forestry inventory data. *Sci. Silvae Sinicae.* **2011**, *47*, 7–12.
14. Li, H.; Zhao, P.; Lei, Y.; Zeng, W. Comparison on estimation of wood biomass using forest inventory data. *Sci. Silvae Sinicae.* **2012**, *48*, 44–52.
15. Yin, H.; Li, H. Comparison of the methods estimating forest biomass based on stock volume. *Forest Res.* **2014**, *27*, 848–853.
16. Jagodziński, A.M.; Dyderski, M.K.; Gęsikiewicz, K.; Horodecki, P. Effects of stand features on above-ground biomass and biomass conversion and expansion factors based on a *Pinus sylvestris* L. chronosequence in Western Poland. *Eur. J. For. Res.* **2019**, *138*, 673–683. [CrossRef]
17. IPCC. *Good Practice for Land Use, Land-Use Change and Forestry*; IPCC/IGES: Hayama, Japan, 2003.
18. IPCC. *IPCC Guidelines for National Greenhouse Gas Inventories—Agriculture, Forestry and Other Land Use*; IPCC/IGES: Hayama, Japan, 2006; Volume 4.
19. Bi, H.; Long, Y.; Turner, J.; Lei, Y.; Snowdon, P.; Li, Y.; Ximenes, F. Additive prediction of above-ground biomass for *Pinus radiata* (D. Don) plantations. *For. Ecol. Manag.* **2010**, *259*, 2301–2314. [CrossRef]
20. Paré, D.; Bernier, P.; Lafleur, B.; Titus, B.D.; Thiffault, E.; Maynard, D.G.; Guo, X. Estimating stand-scale biomass, nutrient contents, and associated uncertainties for tree species of Canadian forests. *Can. J. For. Res.* **2013**, *43*, 599–608. [CrossRef]

21. Dong, L.; Zhang, L.; Li, F. Evaluation of stand biomass estimation methods for major forest types in the eastern Da Xing'an Mountains, Northeast China. *Forests* **2019**, *10*, 715. [CrossRef]
22. Fang, J.; Wang, G.; Liu, G.; Xu, S. Forest biomass of China: An estimate based on the biomass–volume relationship. *Ecol. Appl.* **1998**, *8*, 1084–1091.
23. Brown, S. Aboveground Biomass Estimates for Tropical Moist Forests of Brazilian Amazon. *Interciencia* **1992**, *17*, 8–18.
24. Guo, Z.; Fang, J.; Pan, Y.; Birdsey, R. Inventory-based estimates of forest biomass carbon stocks in China: A comparison of three methods. *For. Ecol. Manag.* **2010**, *259*, 1225–1231. [CrossRef]
25. Schroeder, P.; Brown, S.; Mo, J.; Birdsey, R.; Cieszewski, C. Biomass estimation for temperate broadleaf forests of the United States using inventory data. *For. Sci.* **1997**, *43*, 424–434.
26. Zhou, G.; Wang, Y.; Jiang, Y.; Yang, Z. Estimating biomass and net primary production from forest inventory data: A case study of China's *Larix* forests. *For. Ecol. Manag.* **2002**, *169*, 149–157. [CrossRef]
27. Ketterings, Q.M.; Coe, R.; Van Noordwijk, M.; Palm, C.A. Reducing uncertainty in the use of allometric biomass equations for predicting above-ground tree biomass in mixed secondary forests. *For. Ecol. Manag.* **2001**, *146*, 199–209. [CrossRef]
28. Niklas, K.J. *Plant Allometry: The Scaling of Form and Process*; University of Chicago Press: Chicago, IL, USA, 1994.
29. Monserud, R.A.; Onuchin, A.A.; Tchebakova, N.M. Needle, crown, stem, and root phytomass of *Pinus sylvestris* stands in Russia. *For. Ecol. Manag.* **1996**, *82*, 59–67. [CrossRef]
30. Tang, S.; Li, X.; Meng, Z. The development of studies on stand growth models. *For. Res.* **2012**, *6*, 672–679. (In Chinese)
31. Ou, G.; Xu, H. A Review on Forest Biomass Models. *J. Southwest For. Univ. (Nat. Sci.)* **2020**, *40*, 1–10. (In Chinese)
32. Lehtonen, A.; Cienciala, E.; Tatarinov, F.; Mäkipää, R. Uncertainty estimation of biomass expansion factors for Norway spruce in the Czech Republic. *Ann. For. Sci.* **2007**, *64*, 133–140. [CrossRef]
33. McRoberts, R.E.; Westfall, J.A. Effects of uncertainty in model predictions of individual tree volume on large area volume estimates. *For. Sci.* **2014**, *60*, 34–42. [CrossRef]
34. Zeng, W. *Methodology on Modeling of Single-Tree Biomass Equations for National Biomass Estimation in China*; Chinese Academy of Forestry: Beijing, China, 2011. (In Chinese)
35. Xue, C.; Xu, Q.; Lin, L.; Luo, Y.; Zhao, H.; Lei, Y. Biomass growth models for individual tree of main indigenous broadleaf tree species in Guangdong Province. *J. S. China Agric. Univ.* **2019**, *40*, 65–75. (In Chinese)
36. Cao, Q.V. Evaluation of methods for modeling individual tree survival. *For. Sci.* **2017**, *63*, 356–361. [CrossRef]
37. Chamshama, S.A.O.; Mugasha, A.G.; Zahabu, E. Stand biomass and volume estimation for Miombo woodlands at Kitulangalo, Morogoro, Tanzania. *South. Afr. For. J.* **2004**, *200*, 59–70. [CrossRef]
38. Jagodziński, A.M.; Dyderski, M.K.; Gęsikiewicz, K.; Horodecki, P.; Cysewska, A.; Wierczyńska, S.; Maciejczyk, K. How do tree stand parameters affect young Scots pine biomass? Allometric equations and biomass conversion and expansion factors. *For. Ecol. Manag.* **2018**, *409*, 74–83. [CrossRef]
39. Jagodziński, A.M.; Dyderski, M.K.; Gęsikiewicz, K.; Horodecki, P. Tree-and stand-level biomass estimation in a *Larix decidua* Mill. Chronosequence. *Forests* **2018**, *9*, 587. [CrossRef]
40. Jagodziński, A.M.; Dyderski, M.K.; Gęsikiewicz, K.; Horodecki, P. Tree and stand level estimations of *Abies alba* Mill. above-ground biomass. *Ann. For. Sci.* **2019**, *76*, 56. [CrossRef]
41. Cao, Q.V. Linking individual-tree and whole-stand models for forest growth and yield prediction. *For. Ecosyst.* **2014**, *1*, 18. [CrossRef]
42. Weiskittel, A.R.; Hann, D.W.; Kershaw, J.A., Jr.; Vanclay, J.K. *Forest Growth and Yield Modeling*; John Wiley and Sons: Hoboken, NJ, USA, 2011.
43. Harrison, W.C.; Daniels, R.F. *A New Biomathematical Model for Growth and Yield of Loblolly Pine Plantations*; USDA Forest Service General Technical Report NC-North Central Forest Experiment Station (USA); USDA Forest Service: Washington, DC, USA, 1988.
44. Matney, T.G.; Belli, K.L.; Farrar, R.M., Jr. Parameter-free diameter-distribution recovery. In Division 4, Proceedings of the IUFRO World Congress Meeting, Montréal, QC, Canada, 5–11 August 1990; pp. 5–11.
45. Qin, J.; Cao, Q.V. Using disaggregation to link individual-tree and whole-stand growth models. *Can. J. For. Res.* **2006**, *36*, 953–960. [CrossRef]
46. García, O. On bridging the gap between tree-level and stand-level models. In Proceedings of the IUFRO 4.11 Conference "Forest Biometry, Modelling and Information Science", London, UK, 25–29 June 2001; pp. 25–29.
47. Hevia, A.; Cao, Q.V.; Álvarez-González, J.G.; Ruiz-González, A.D.; Gadow, K.V. Compatibility of whole-stand and individual-tree models using composite estimators and disaggregation. *For. Ecol. Manag.* **2015**, *348*, 46–56. [CrossRef]
48. Ou, G.; Li, C.; Lv, Y.; Wei, A.; Xiong, H.; Xu, H.; Wang, G. Improving above-ground biomass estimation of *Pinus densata* forests in Yunnan using Landsat 8 imagery by incorporating age dummy variable and method comparison. *Remote Sens.* **2019**, *11*, 738. [CrossRef]
49. Xu, D.; Zhang, J.; Bao, R.; Liao, Y.; Han, D.; Liu, Q.; Cheng, T. Temporal and Spatial Variation of Aboveground Biomass of *Pinus densata* and Its Drivers in Shangri-La, CHINA. *Int. J. Environ. Res. Public Health* **2021**, *19*, 400. [CrossRef]
50. Cheng, X.; Wang, Y.; Li, W.; Gong, H.; Wang, S.; Wang, S. Effects of spatial autocorrelation on individual tree growth model of *Picea likiangensis* forest in northwest of Yunnan, China. *J. Anim. Plant Sci.* **2015**, *25*, 1411–1418.
51. Li, F.R. *Forest Mensuration*, 4th ed.; Chinese Forestry Publishing House: Beijing, China, 2019.
52. Zeng, W.; Duo, H.; Lei, X.; Chen, X.; Wang, X.; Pu, Y.; Zou, W. Individual tree biomass equations and growth models sensitive to climate variables for Larix spp. in China. *Eur. J. For. Res.* **2017**, *136*, 233–249. [CrossRef]

53. Zianis, D.; Muukkonen, P.; Mäkipää, R.; Mencuccini, M. Biomass and stem volume equations for tree species in Europe. In *Silva Fennica (Monographs 4)*; Tammer-Paino Oy: Tampere, Finland, 2005; 63p.
54. Zeng, W.; Tang, S. Modeling compatible single-tree above-ground biomass equations of Masson pine (*Pinus massoniana*) in southern China. *J. For. Res.* **2012**, *23*, 593–598. [CrossRef]
55. R Core Team. *R: A Language and Environment for Statistical Computing*; R Foundation for Statistical Computing: Vienna, Austria, 2018.
56. Guo, X.; Feng, Z.; Cao, Z.; Fan, Y. Tree Height Measure Model Based on 1stOpt Software. *J. Northeast For. Univ.* **2015**, *43*, 38–41, 83. (In Chinese)
57. Zeng, W.S. Integrated individual tree biomass simultaneous equations for two larch species in northeastern and northern China. *Scand. J. For. Res.* **2015**, *30*, 594–604. [CrossRef]
58. Zeng, W.S. Using nonlinear mixed model and dummy variable model approaches to develop origin-based individual tree biomass equations. *Trees* **2014**, *29*, 275–283. [CrossRef]
59. Pallant, J. *SPSS Survival Manual: A Step by Step Guide to Data Analysis using IBM SPSS*; Routledge: Milton Park, UK,, 2020.
60. Skovsgaard, J.P.; Nord-Larsen, T. Biomass, basic density and biomass expansion factor functions for European beech (*Fagus sylvatica* L.) in Denmark. *Eur. J. For. Res.* **2012**, *131*, 1035–1053. [CrossRef]
61. Jagopziński, A.M.; Oleksyn, J. Ecological consequences of silviculture at variable stand densities. II. Biomass production and allocation, nutrient retention. *Sylwan* **2009**, *153*, 147–157.
62. Gavrikov, V.L. A theory to link relationships of stand volume, density, mean diameter and height in forestry data. *J. For. Res.* **2021**, *32*, 15–20. [CrossRef]
63. Fang, J.; Chen, A.; Peng, C.; Zhao, S.; Ci, L. Changes in forest biomass carbon storage in China between 1949 and 1998. *Science* **2001**, *292*, 2320–2322. [CrossRef] [PubMed]
64. Zeng, W.; Sun, X.; Wang, L.; Wang, W.; Pu, Y. Developing stand volume, biomass and carbon stock models for ten major forest types in forest region of northeastern China. *J. Beijing For. Univ.* **2021**, *43*, 1–8. (In Chinese)
65. Usoltsev, V.A.; Shobairi, S.O.R.; Chasovskikh, V.P. Triple harmonization of transcontinental allometric of *Picea* spp. and *Abies* spp. forest stand biomass. *Ecol. Environ. Conserv.* **2018**, *24*, 1966–1972.
66. Peichl, M.; Arain, M.A. Allometry and partitioning of above- and belowground tree biomass in an age-sequence of white pine forests. *For. Ecol. Manag.* **2007**, *253*, 68–80. [CrossRef]
67. Kauppi, P.E.; Tomppo, E.; Ferm, A. C and N storage in living trees within Finland since 1950s. *Plant Soil* **1995**, *168*, 633–638. [CrossRef]
68. Lehtonen, A.; Mäkipää, R.; Heikkinen, J.; Sievänen, R.; Liski, J. Biomass expansion factors (BEFs) for Scots pine, Norway spruce and birch according to stand age for boreal forests. *For. Ecol. Manag.* **2004**, *188*, 211–224. [CrossRef]
69. Jagodziński, A.M.; Zasada, M.; Bronisz, K.; Bronisz, A.; Bijak, S. Biomass conversion and expansion factors for a chronosequence of young naturally regenerated silver birch (*Betula pendula* Roth) stands growing on post-agricultural sites. *For. Ecol. Manag.* **2017**, *384*, 208–220. [CrossRef]
70. Wirth, C.; Schumacher, J.; Schulze, E.D. Generic biomass functions for Norway spruce in Central Europe—A meta-analysis approach toward prediction and uncertainty estimation. *Tree Physiol.* **2004**, *24*, 121–139. [CrossRef]
71. Jia, W.; Sun, H.; Li, F. Prediction model system with dummy variables for carbon storage of larch plantation in Heilongjiang Province, China. *Chin. J. Appl. Ecol.* **2019**, *30*, 814–822. (In Chinese)
72. He, X.; Zhou, C.; Lei, X.; Li, H. Stand carbon stock growth model system for *Larix olgensis* plantation. *J. Beijing For. Univ.* **2021**, *43*, 1–10. (In Chinese)
73. Wertz, B.; Bembenek, M.; Karaszewski, Z.; Ochał, W.; Skorupski, M.; Strzeliński, P.; Mederski, P.S. Impact of Stand Density and Tree Social Status on Aboveground Biomass Allocation of Scots Pine *Pinus sylvestris* L. *Forests* **2020**, *11*, 765. [CrossRef]
74. Jagodziński, A.M.; Oleksyn, J. Ecological consequences of silviculture at variable stand densities. I. Stand growth and development. *Sylwan* **2009**, *153*, 75–85.
75. Jalkanen, A.; Mäkipää, R.; Ståhl, G.; Lehtonen, A.; Petersson, H. Estimation of the biomass stock of trees in Sweden: Comparison of biomass equations and age-dependent biomass expansion factors. *Ann. For. Sci.* **2005**, *62*, 845–851. [CrossRef]
76. Mabvurira, D.; Miina, J. Individual-tree growth and mortality models for *Eucalyptus grandis* (Hill) Maiden plantations in Zimbabwe. *For. Ecol. Manag.* **2002**, *161*, 231–245. [CrossRef]
77. Reineke, L.H. Perfecting a stand-density index for even-aged forests. *J. Agric. Res.* **1933**, *46*, 627–638.
78. Xu, W.; Jin, X.; Liu, J.; Yang, X.; Ren, J.; Zhou, Y. Analysis of spatio-temporal changes in forest biomass in China. *J. For. Res.* **2022**, *33*, 261–278. [CrossRef]
79. Jiang, X.; Yang, J.; Liu, Y. A study on the growth and yield model of prediction for papermaking and raw material stand of *Masson Pine*. *J. Fujian Coll. For.* **2001**, *21*, 1–5. (In Chinese)
80. Luis, J.F.S.; Fonseca, T.F. The allometric model in the stand density management of *Pinus pinaster* Ait. in Portugal. *Ann. For. Sci.* **2004**, *61*, 807–814. [CrossRef]
81. Zhang, X.; Cao, Q.V.; Lu, L.; Wang, H.; Duan, A.; Zhang, J. Use of modified Reineke's stand density index in predicting growth and survival of Chinese fir plantations. *For. Sci.* **2019**, *65*, 776–783. [CrossRef]
82. Zavitkovski, J. Dry weight and leaf area of aspen trees in northern Wisconsin. *Maine Agr. Exp. Sta. Misc. Rep.* **1971**, *132*, 193–205.
83. Saint-André, L.; M'Bou, A.T.; Mabiala, A.; Mouvondy, W.; Jourdan, C.; Roupsard, O.; Nouvellon, Y. Age-related equations for above-and below-ground biomass of a *Eucalyptus* hybrid in Congo. *For. Ecol. Manag.* **2005**, *205*, 199–214. [CrossRef]

84. Xue, C.; Xu, Q.; Lin, L.; He, X.; Luo, Y.; Zhao, H.; Cao, L.; Lei, Y. Biomass Models with Breast Height Diameter and Age for Main Native tree Species in Guangdong Province. *Sci. Silvae Sin.* **2019**, *55*, 97–108. (In Chinese)
85. Cao, L.; Liu, X.; Li, H.; Lei, Y. Biomass Growth Models for Evergreen Broad-leaved Forests in Guangdong. *For. Res.* **2020**, *33*, 61–67. (In Chinese)